Journal of Magnetism and Magnetic Materials 394 (2015) 138–142

Contents lists available at ScienceDirect

Journal of Magnetism and Magnetic Materials

journal homepage: www.elsevier.com/locate/jmmm

An X-band Co^{2+} EPR study of $Zn_{1-x}Co_xO$ ($x=0.005$–0.1) nanoparticles prepared by chemical hydrolysis methods using diethylene glycol and denaturated alcohol at 5 K

Sushil K. Misra [a,*], S.I. Andronenko [b], S. Srinivasa Rao [c], Jordan Chess [c], A. Punnoose [c]

[a] Physics Department, Concordia University, Montreal, QC, Canada H3G 1M8
[b] Physics Institute, Kazan Federal University, Kazan 420008, Russian Federation
[c] Department of Physics, Boise State University, Boise, ID 83725-1570, USA

ARTICLE INFO

Article history:
Received 9 January 2015
Received in revised form
22 June 2015
Accepted 23 June 2015
Available online 25 June 2015

Keywords:
EPR
Nanoparticle
ZnO
Dilute magnetic semiconductor
Co^{2+} ion

ABSTRACT

EPR investigations on two types of dilute magnetic semiconductor (DMS) ZnO nanoparticles doped with 0.5–10% Co^{2+} ions, prepared by two chemical hydrolysis methods, using: (i) diethylene glycol ($(CH_2CH_2OH)_2O$) (NC-rod-like samples), and (ii) denatured ethanol (CH_3CH_2OH) solutions (QC-spherical samples), were carried out at X-band (9.5 GHz) at 5 K. The analysis of EPR data for NC samples revealed the presence of several types of EPR lines: (i) two types, intense and weak, of high-spin Co^{2+} ions in the samples with Co concentration $>0.5\%$; (ii) surface oxygen vacancies, and (iii) a ferromagnetic resonance (FMR) line. QC samples exhibit an intense FMR line and an EPR line due to high-spin Co^{2+} ions. FMR line is more intense, than the corresponding line exhibited by NC samples. These EPR spectra varied for sample with different doping concentrations. The magnetic states of these samples as revealed by EPR spectra, as well as the origin of ferromagnetism DMS samples are discussed.

1. Introduction

Dilute magnetic semiconductors (DMS), lightly doped with transition-metal (TM) ions, exhibit novel magnetic and electrical properties. They possess room-temperature ferromagnetism and characterized by a rather high conductivity, rendering them potential spintronic devices. Co^{2+} -doped ZnO nanoparticles are prospective DMS candidates, and have been investigated extensively [1–25]. EPR studies of the Co^{2+} ion in magnetic semiconductors, such as SnO_2 [26], provide information on the magnetic state of this compound, and its behavior under different synthesis conditions [1,16–25]. The main conclusions of these investigations are: (i) there are present both localized Co^{2+} ions and ferromagnetically coupled Co^{2+} ions in the host material; (ii) The spin-Hamiltonian (SH) parameters for the Co^{2+} ion are very close to those for Co^{2+}-substituted ZnO crystal, characterized by high-spin Co^{2+} ions; (iii) there is exhibited an electron paramagnetic resonance (EPR) signal due to Co^{2+} ions, situated in distorted local environment, characterized by high-spin Co^{2+} ions.

ZnO is a semiconductor with the energy gap of 3.3 eV, which can be increased by introducing different impurities up to 4 eV [27]. Magnetic properties, X-ray photoelectron spectroscopy, EPR, and photoluminescence study of ZnO nanoparticles, doped with Co ions, prepared using the acetate method, were recently reported [1]. It is the purpose of the present paper to report detailed X-band (9.5 GHz) EPR investigations at 5 K on two types of ZnO nanoparticles, NC and QC, doped with 0.5%, 2.5%, 5%, 10% Co^{2+} ions, prepared from two different solutions. The present study is aimed to estimate the spin-Hamiltonian parameters of the Co^{2+} ions in NC and QC samples, and to find the reasons for different magnetization observed in NC and QC samples, and the origin of ferromagnetism in these samples.

2. Sample preparation and structure

NC and QC samples of $Zn_{1-x}Co_xO$ nanoparticles, doped with Co^{2+} ions, with $x=0.005$, 0.025, 0.05, 010, were prepared using chemical hydrolysis methods [1] using: (i) diethylene glycol ($(CH_2CH_2OH)_2O$) (NC-rod-like samples [28], referred to as NC hereafter), and (ii) denatured ethanol (CH_3CH_2OH) solutions (QC-spherical samples [29], referred to as QC hereafter).

X-ray diffraction (XRD) was employed to investigate the structural properties and crystal size, as well as to rule out the presence of undesired impurity phases. The structure and purity of NC samples has been discussed in detail in [1]. The average size of

* Corresponding author.
E-mail address: skmisra@alcor.concordia.ca (S.K. Misra).

http://dx.doi.org/10.1016/j.jmmm.2015.06.063
0304-8853/

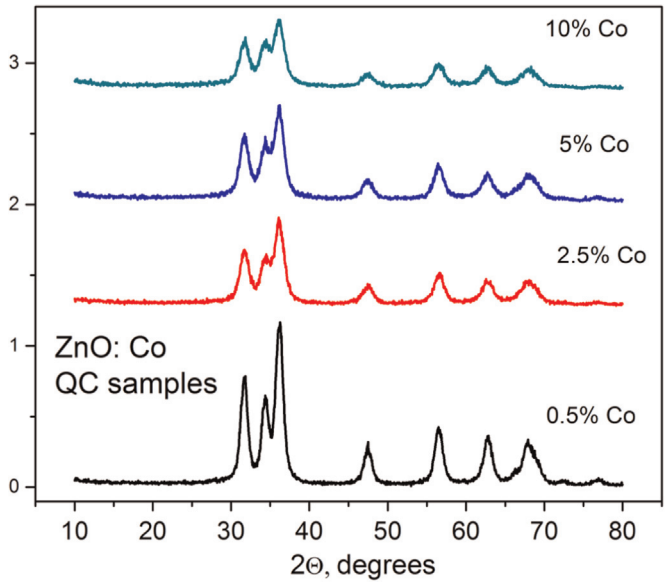

Fig. 1. XRD pictures for nanoparticles of ZnO, doped with Co, QC samples.

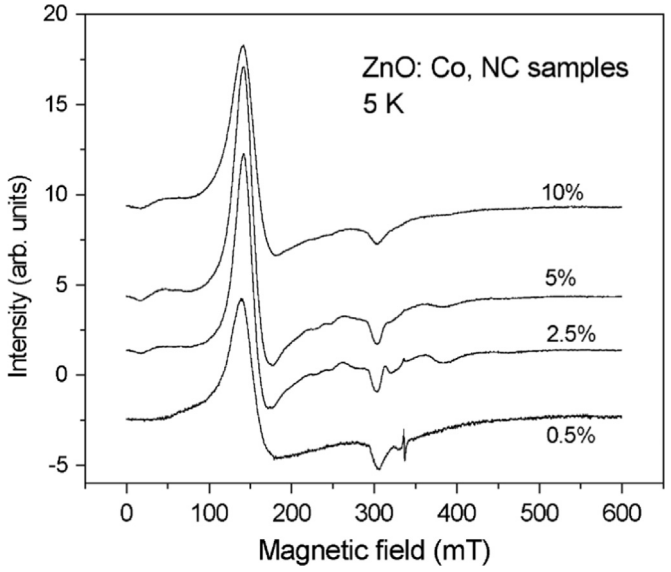

Fig. 2. X-band (9.4 GHz) Co^{2+} EPR spectra of ZnO nanoparticles in NC samples doped with different concentrations of Co ions at 5 K.

nanoparticles of ZnO in NC samples is about 9 nm according to [1]. The XRD patterns for QC samples are shown at Fig. 1. These pictures confirm the absence of secondary phases in large nanoparticles. The XRD patterns showed only the crystalline Wurtzite ZnO phase, with the space-group symmetry C_{6v}^4 and the point-group symmetry C_{3v} at the site of Zn [30]. Since the ionic radii of Co^{2+} (0.72 Å) and Zn^{2+} (0.74 Å) are almost the same, the Co^{2+} ion is characterized by the same point-group symmetry at the substitutional position C_{3v}, as seen by the Zn^{2+} ion.

3. EPR spectra

X-band spectra were recorded using the commercial X-band Bruker Elexsys E500 spectrometer, operating at 9.414 GHz, at Boise State University, Boise, ID USA. The EPR spectrometer settings were: modulation 1 G, mw power 30 dB. An Oxford Instrument helium gas-flow cryostat was used for low temperature measurements. The observed EPR spectra at 5 K for NC and QC samples with different Co concentrations are shown in Figs. 1 and 2, respectively. Ferromagnetic and paramagnetic EPR signals were observed in both samples. It is noted that due to EPR lines being rather broad, the Co^{2+} hyperfine splitting into 8 lines for nuclear spin $I=7/2$ is not resolved in any spectrum. The details of the EPR spectra are follows.

3.1. NC samples (Fig. 2)

Simulations of EPR spectra revealed that the overall spectrum for NC samples consists of an overlap of four spectra: (i) an intense high-spin (HS) Co^{2+} spectrum; (ii) a V_O (oxygen vacancy) spectrum; (iii) a weak HS Co^{2+} EPR spectrum; (iv) a FMR (ferromagnetic resonance spectrum). The EPR spectra were broadened due to crystal-field disorder in all NC nanoparticles for $x=0.5\%$, 2.5%, 5%, 10%. This disorder is caused by the oxygen vacancies in the second co-ordination sphere of the Co^{2+} ion which leads to a distribution of zero field parameter D. The EPR line near $B\approx 336$ mT with $g=2.003$ in Fig. 1 is due to the well-known surface oxygen vacancies [31–33]. The very broad FMR signal was found by simulation to be centered at about 370 mT, with the linewidth $\Delta B=120$ mT. The intensity of the FMR line changed with the concentration, x, with the maximum value occurring for

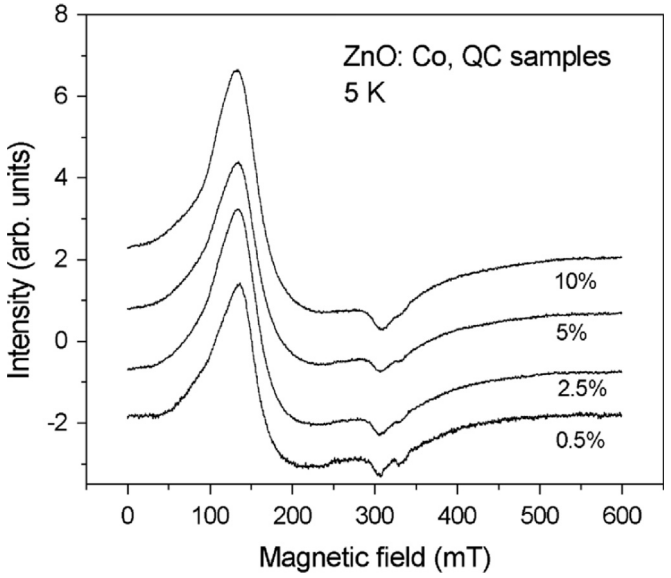

Fig. 3. X-band (9.4 GHz) Co^{2+} EPR spectra of ZnO nanoparticles in QC samples doped with different concentrations of Co ions at 5 K.

$x=0.1$ Co.

3.2. QC samples (Fig. 3)

As for QC samples, only a high-spin (HS) EPR spectrum, in addition to an FMR line is observed. The HS spectrum is similar to the intense high-spin EPR spectrum for NC samples, but it is much broader. The integrated intensity of the FMR signal in QC samples is larger than that for the NC samples. There is present an additional weak EPR line near $B\approx 327$ mT in QC samples, which was interpreted as HS2 Co^{2+} spectrum, similar to that for NC samples.

It is noted that for both samples, NC and QC, the integrated intensity increases with increasing Co-ion concentration up to 2.5% Co. It slowly decreases above this concentration, as was reported in [1] for NC samples. It means that a fraction of Co^{2+} ions transform to EPR-silent Co^{3+} above the threshold of 2.5% Co concentration. This conclusion was confirmed by XPS (X-ray photoelectron spectroscopy) spectra for NC samples [1].

4. Simulation of EPR spectra

To interpret the experimental results, EPR spectra were simulated by diagonalization of the spin-Hamiltonian matrix for various choices of spin-Hamiltonian parameters (SHP) by using the SPIN software to find the best agreement of the simulated spectrum with the experimental one. These SHP which provide the best agreement help to identify the sites at which the various Co ions are located in these samples.

In these samples, Co^{2+} ions, with the configuration ($3d^7$, ^4F), normally substitute for Zn^{2+} ions, in tetrahedral coordination in the ZnO Wurtzite structure. The parameters for isolated Co^{2+} ($S=3/2$) ions in ZnO single crystals, as reported by Estle and De Wit [34] and by Koidl [35] are: $g_{||}=2.23$, $g_{\perp}=2.27$, $D=2.7\ cm^{-1}$, $A_{||}=16\times10^{-4}\ cm^{-1}$, $A_{\perp}=3\times10^{-4}\ cm^{-1}$, which can be used as initial parameters in the simulations here.

The high-spin Co^{2+} X-band powder EPR spectra (HS1) for NC and QC samples is here simulated with $S=3/2$, using the axial spin-Hamiltonian (SH) [36,37]:

$$H = \mu_B gB.\ S + S.\ A.\ I + D\left[S_z^2 - \tfrac{1}{3}S(S+1)\right], \quad (1)$$

In Eq. (1), μ_B is the Bohr magneton; S ($=3/2$) is the electronic spin of the Co^{2+} ion; B is the external magnetic field; A is hyperfine interaction tensor; and $I=7/2$ is the nuclear spin for the Co^{2+} ion. The constant A cannot be determined because of non-observance of hyperfine splitting due to large line broadening of the spectra, so not included in the simulations.

For NC samples with $x=0.025$, 0.05, 0.1 Co, there is observed an additional spectrum. This high-spin (HS2) EPR spectrum is due to those Co^{2+} ions, which are situated in a highly distorted environment, most likely near the nanoparticle surface in interstitial positions.

In addition to HS1 and HS2 spectra, there was also present surface oxygen-defect (V_O) spectrum, characterized by $S=1/2$ in NC samples. For these, the same SH as described by Eq. (1), but without the hyperfine term and zero-field splitting term, is applicable.

The experimental and simulated Co^{2+} EPR spectra at X-band at 5 K in NC sample with Co^{2+} concentration of 2.5% are shown in Fig. 4, whereas those for QC sample with Co^{2+} concentration of 2.5% in Fig. 5.

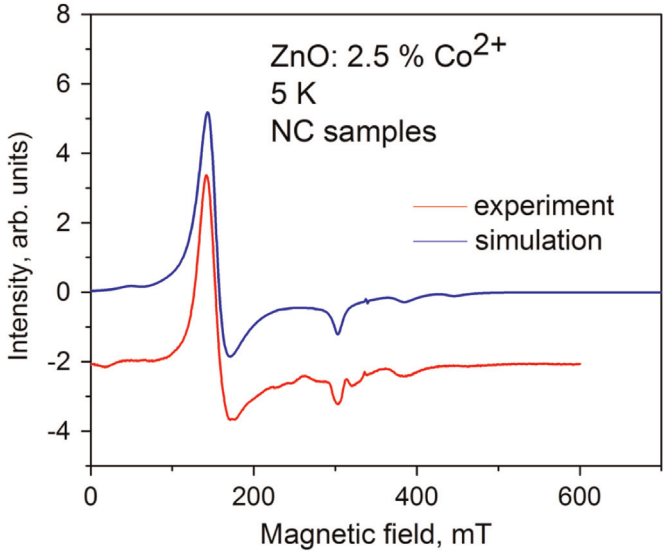

Fig. 4. The observed X-band EPR spectrum at 5 K and simulated Co^{2+} EPR spectra (NC samples) in nanoparticles of ZnO, doped with 2.5% Co. The simulated spectrum has been displaced upward for comparison.

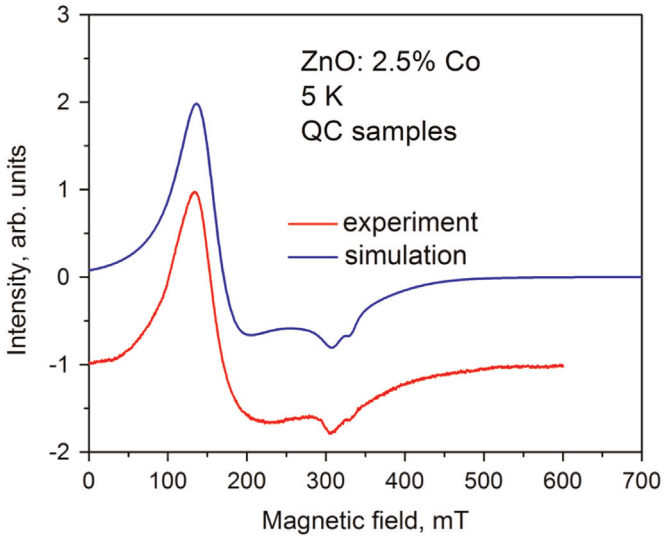

Fig. 5. The observed X-band EPR spectrum at 5 K and simulated Co^{2+} EPR spectra (QC samples) in nanoparticles of ZnO, doped with 2.5% Co. The simulated spectrum has been displaced upward for comparison.

Table 1
Spin-Hamiltonian parameters for Co^{2+} in ZnO NC sample doped with 2.5% Co at X-band. ΔB_x, ΔB_y, ΔB_z denote the peak-to-peak linewidth used in simulation.

$Zn_{1-x}Co_xO$	g_x, g_y	g_z	ΔB_x, ΔB_y (mT)	ΔB_z (mT)	D (mT)	Relat. intens.
High spin 1 $S=3/2$ Co^{2+}	2.31	2.24	19.0	8.0	2900	1
High spin 2 $S=3/2$ Co^{2+}	2.5	2.45	20.0	20.0	230.0	0.08
Surface oxygen defect (V_O) $S=1/2$	2.00	2.00	2.0	2.0		0.02
FMR	2.8	2.8	120.0	120.0		0.08

Table 2
Spin-Hamiltonian parameters for Co^{2+} in ZnO QC sample doped with 2.5% Co at X-band. ΔB_x, ΔB_y, ΔB_z denote the peak-to-peak linewidth used in simulation.

$Zn_{1-x}Co_xO$	g_x, g_y	g_z	ΔB_x, ΔB_y (mT)	ΔB_z (mT)	D (mT)	Relat. intens.
High Spin 1 $S=3/2$ Co^{2+}	2.30	2.18	40.0	20.0	2900	1.0
High Spin 2 $S=3/2$ Co^{2+}	2.03	2.03	44.0	10.0	2000	0.23
FMR	2.86	2.86	160.0	160.0		0.25

4.1. Simulation parameters

The best-fit SH parameters are listed in Tables 1 and 2 for NC and QC samples, respectively. The shape of HS EPR line used for simulations is 100% Lorentzian. The shape of FMR line is Gaussian. The simulation for NC samples revealed the following: (i) the main Co^{2+} EPR spectrum in NC and QC samples is characterized by HS1 SH parameters, which are close to those for Co^{2+} in ZnO single crystal. This is due to those Co^{2+} ions, which are situated in the core area of the nanoparticle; (ii) there were present low-intensity HS2 EPR signals in both NC and QC samples with Co concentrations more than 0.05; (iii) there was present an EPR spectrum only in NC samples due to surface oxygen vacancies, possessing specific g-value $g=2.00$; and (iv) there was observed an FMR line from ferromagnetically ordered part in ZnO nanoparticles in both NC and QC samples.

A distribution of orthorhombic D parameter can contribute to

the broadening of Co^{2+} HS1 EPR spectra [38].

5. Ferromagnetism

The origin of ferromagnetism in DMS compounds is not yet fully understood. There have been proposed two mechanisms for it: (i) indirect interaction of impurity ions via oxygen ions, oxygen vacancies, and color centers (also referred to as F-centers, which are oxygen vacancies with trapped electrons) [39–41]; (ii) electron transfer in defect oxides, wherein ferromagnetism arises from defect-band electron structure of semiconducting ZnO as explained by the model of Stoner ferromagnetism [42].

The ferromagnetic behavior of NC samples of ZnO nanoparticles, doped with Co ions, was investigated in detail in [1] at room temperature. The magnetic moment of ZnO nanoparticles, doped with Co, was measured using a vibrational sample magnetometer. The magnetization was accurately adjusted, taking into account the diamagnetism of the piece of straw on which the magnetic powder was placed, and the mass of each sample. The room-temperature dependence of magnetization on the magnetic field and the dependence of the ferromagnetic part of the magnetization on the magnetic field are shown in Fig. 6a and b, respectively. It is clearly observed, that these QC samples exhibit ferromagnetic behavior with hardly any hysteresis, similar to the behavior of NC samples [1]. The maximum of saturation magnetization was observed for the sample with 2.5% Co concentration, the same concentration for which the maximum Co^{2+} EPR integrated intensity was observed. It is clear from Fig. 6b that the main contribution to the magnetization is due to the paramagnetic part of the magnetization, because of its mainly linear dependence on magnetic field. This maximum of saturation magnetization (0.003 emu/g) for the sample with $x=0.25$ is very close to that observed in NC samples [1]. Further increase in Co concentration leads to a decrease in the number of doubly ionized (Co^{2+}) ions and an increase in the triply ionized (Co^{3+}) ions. As seen from Fig. 6b, the saturation magnetizations of the samples with Co concentrations of 5% and 10% are much less than that for the sample with the concentration of 2.5%. This implies that only Co^{2+} ions are involved in the ferromagnetic ordering of ZnO nanoparticles. As one can see, both EPR and magnetization studies provide similar results, namely that the predominant magnetization is due to the paramagnetic part, which is contributed by the isolated Co^{2+} ions; the ferromagnetic part of magnetization is insignificant. Furthermore, this ferromagnetic part of magnetization is slightly larger in QC samples, as compared to that in NC samples.

There is still some discussion on the nature of the ferromagnetic behavior of nanoparticles of ZnO doped with Co. A theoretical study of this problem [43] denies the possibility of existence of itinerant (long-range) ferromagnetism in this system. Such magnetic behavior, that is the superparamagnetic behavior with ferromagnetic interaction between Co ions, is here attributed to the presence of nanoparticles of metallic Co or Co_2O_3 particles with very small size, 1–2 nm, which was really observed in these ZnO nanoparticles [12]. Volbers et al. [19] did not find ferromagnetism in ZnO:Co nanoparticles. XRD study cannot detect any secondary phases unambiguously for such small particles, and if nanoparticles are small enough, they are not detected by XRD. On the other hand, many experimental investigations suggest the existence of a long-range ferromagnetic exchange interaction in ZnO:Co nanoparticles [44,45]. Direct confirmation of such probability was found in ZnO crystals doped with Co^{2+} ion, where Co^{2+}–Co^{2+} dimer centers were found, in which Co^{2+} ions are weakly ferromagnetically coupled. This was explained by invoking the mechanism involving additional defects, e.g. singly charged oxygen vacancies [25]. Another possibility for the existence of ferromagnetically coupled Co^{2+} ions in this nanoparticles was pointed out in [6], where the competition of two Co ions population occurred: one with antiferromagnetic interaction between Co ions and the other with ferromagnetic interaction. Finally it leads to superparamagnetic behavior, caused by a ferromagnetic interaction, within clusters of Co ions, resulting in both-paramagnetic and superparamagnetic behaviors of magnetizations of nanoparticles of ZnO, doped with Co ions.

6. Conclusions

The salient features of the present X-band EPR investigations at 5 K on Co^{2+} in NC and QC ZnO nanoparticles are as follows:

(1) The observed EPR spectra provide clear evidence for the presence of both paramagnetic Co^{2+} ions exhibiting sharp lines, and ferromagnetically coupled ions, exhibiting very broad FMR lines. The study of magnetization proves this conclusion convincingly, that there are paramagnetic and ferromagnetic (superparamagnetic) parts of the magnetization of ZnO

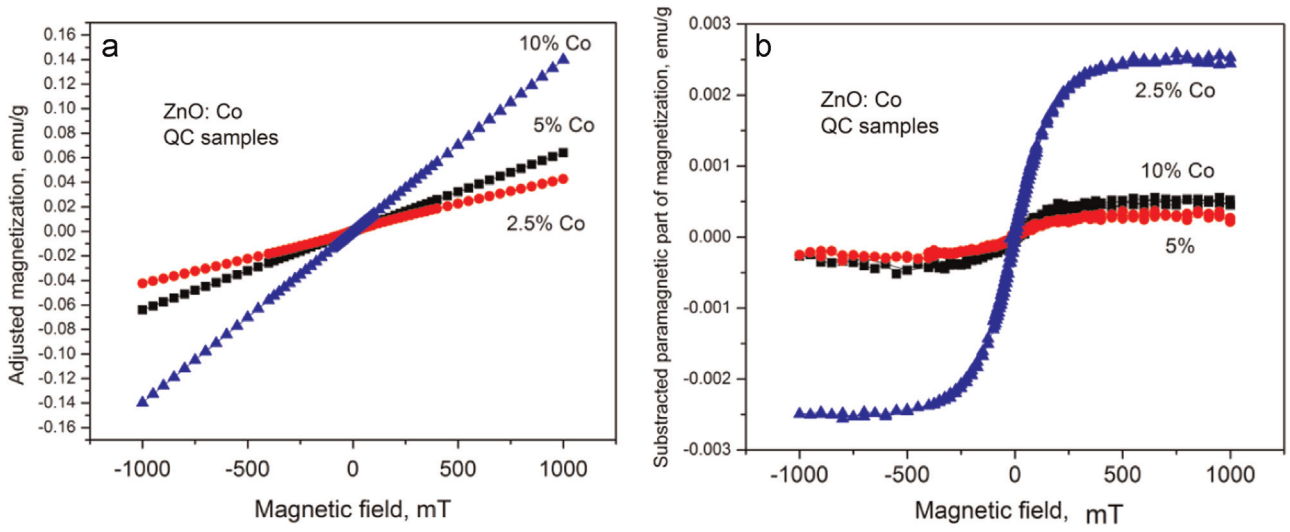

Fig. 6. Magnetization of ZnO nanoparticles, doped with Co ions, QC samples at room temperature. (a) Total magnetization; (b) ferromagnetic part of magnetization.

nanoparticles, doped with Co.

(2) The EPR linewidth of Co^{2+} in QC samples is much larger than that in NC samples.

(3) An EPR signal due to surface oxygen vacancies, was observed in NC samples, but not in QC samples. This explains the smaller magnetic moment in NC samples, where not all the oxygen vacancies are involved in ferromagnetic coupling. QC samples, on the other hand, exhibit strong FMR signals, suggesting that all the oxygen vacancies in them are ferromagnetically coupled.

(4) Use of solvent in preparing nanosamples determines significantly the property of the sample as demonstrated by the different EPR spectra exhibited by NC and QC samples prepared by the use of different solvents.

Acknowledgments

This research was supported by the Natural Sciences and Engineering Research Council of Canada (NSERC, Grant #A4485-SKM); and by the National Science Foundation Grants EAGER DMR-1137419 and CBET 1134468 (AP). SIA also acknowledges the support from the subsidy allocated to Kazan Federal University for performing the state assignment in the area of scientific activities.

References

[1] J. Chess, G. Alanko, D.A. Tenne, Ch.B. Hanna, A. Punnoose, Correlation between magnetism and electronic structure of $Zn_{1-x}Co_xO$ nanoparticles, J. Appl. Phys. 113 (2013) 17C302.

[2] K. Sato, H. Katayama-Yoshida, Stabilization of ferromagnetic states by electron doping in Fe-, Co- or Ni-doped ZnO, Jpn. J. Appl. Phys. 40 (2001) L334–L336.

[3] G. Glaspell, P. Dutta, A. Manivannan, A room-temperature and microwave synthesis of M-doped ZnO (M=Co, Cr, Fe, Mn & Ni), J. Cluster Sci. 16 (2005) 523–536.

[4] L.M. Johnson, A. Thurber, J. Anghel, M. Sabetian, M.H. Engelhard, D.A. Tenne, Ch. B. Hanna, A. Punnoose, Transition metal dopants essential for producing ferromagnetism in metal oxide nanoparticles, Phys. Rev. B 82 (2010) 054419.

[5] K. Sato, H. Katayama-Yoshida, Electronic structure and ferromagnetism of transition metal–impurity-doped zinc oxide, Phys. B: Condens. Matter 308–310 (2001) 904–907.

[6] O. Toulemonde, M. Gaudon, New examination of the magnetic properties of cobalt-doped ZnO diluted magnetic semiconductors, J. Phys. D: Appl. Phys 43 (2010) 045001.

[7] J. Alaria, M. Venkatesan, J.M.D. Coey, Magnetism of ZnO nanoparticles doped with 3*d* cations prepared by a solvothermal method, J. Appl. Phys. 103 (2008) 07D123.

[8] B. Pal, P.K. Gin, High temperature ferromagnetism and optical properties of Co doped ZnO nanoparticles, J. Appl. Phys. 108 (2010) 084322.

[9] B. Martinez, F. Sandiumenge, L.I. Balcells, J. Arbiol, F. Sibieude, C. Monty, Role of the microstructure on the magnetic properties of Co-doped ZnO nanoparticles, Appl. Phys. Lett. 86 (2005) 103113.

[10] P.K. Sharma, R.K. Datta, A.C. Pandey, Alteration of magnetic and optical properties of ultrafine dilute magnetic semiconductor ZnO: Co^{2+} nanoparticles, J. Colloid Interface Sci. 345 (2010) 149–153.

[11] M. Venkatesan, C.B. Fitzgerald, J.G. Lunney, J.M.D. Coey, Anisotropic ferromagnetism in substituted zinc oxide, Phys. Rev. B 93 (2004) 177206.

[12] A. Ney, A. Kov´acs, V. Ney, S. Ye, K. Ollefs, T. Kammermeier, F. Wilhelm, A. Rogalev, R.E. Dunin-Borkowski, Structural, chemical and magnetic properties of secondary phases in Co-doped ZnO, New J. Phys. 13 (2011) 103001.

[13] S. Udayakumar, V. Renuka, K. Kavitha, Structural, optical and thermal studies of cobalt doped hexagonal ZnO by simple chemical precipitation method, J. Chem. Pharm. Res. 4 (2012) 1271–1280.

[14] G.S. Chang, E.Z. Kurmaev, D.W. Boukhvalov, L.D. Finkelstein, S. Colis, T. M. Pedersen, A. Moewes, A. Dinia, Effects of Co and O vacancies on the magnetism in Co-doped ZnO: experiment and theory, Phys. Rev. B 75 (2007) 195215.

[15] K.R. Kittilstved, D.A. Schwartz, A.C. Tuan, S.M. Heald, S.A. Chambers, D. R. Gamelin, Direct kinetic correlation of carriers and ferromagnetism in Co^{2+}: ZnO, Phys. Rev. Lett. 97 (2006) 037203.

[16] G. Clavel, M.-G. Willinger, D. Zitoun, N. Pinna, Solvent dependent shape and magnetic properties of doped ZnO nanostructures, Adv. Funct. Mater. 17 (2007) 3159–3169.

[17] N. Jedrecy, H.J. von Bardelen, Y. Zheng, J.-L. Cantin, Electron paramagnetic resonance study of $Zn_{1-x}Co_xO$: a predicted high-temperature ferromagnetic semiconductor, Phys. Rev. B 69 (2004) 041308.

[18] R. Baraki, P. Zierep, E. Erdem, S. Weber, T. Granzow, Electron paramagnetic resonance study of ZnO varistor material, J. Phys.: Cond. Matter. 26 (2014) 115801.

[19] N. Volbers, H. Zhou, C. Knies, D. Pfisterer, J. Sann, D.M. Hofmann, B.K. Meyer, Synthesis and characterization of ZnO: Co^{2+} nanoparticles, Appl. Phys. A 88 (2007) 153–155.

[20] A.O. Ankiewicz, M.C. Carmo, N.A. Sobolev, W. Gehlhoff, E.M. Kaidashev, A. Rahm, M. Lorenz, M. Grundmann, Electron paramagnetic resonance in transition metal-doped ZnO nanowires, J. Appl. Phys. 101 (2007) 024324.

[21] A.S. Pereira, A.O. Ankiewicz, W. Gehlhoff, A. Hoffmann, S. Pereira, T. Trindade, M. Grundmann, M.C. Carmo, N.A. Sobolev, Surface modification of Co-doped ZnO nanocrystals and its effects on the magnetic properties, J. Appl. Phys. 103 (2008) 07D140.

[22] I. Ozerov, F. Chabre, W. Marine, Incorporation of cobalt into ZnO nanoclusters, Mater. Sci. Eng. C 25 (2005) 614–617.

[23] P. Sati, R. Hayn, R. Kuzian, S. Régnier, S. Schäfer, A. Stepanov, C. Morhain, C. Deparis, M. Laügt, M. Goiran, Z. Golacki, Magnetic anisotropy of Co^{2+} as signature of intrinsic ferromagnetism in ZnO: Co, Phys. Rev. Lett. 96 (2003) 017203.

[24] R.O. Kuzian, A.M. Dake, P. Sati, R. Hayn, Crystal-field theory of Co^{2+} in doped ZnO, Phys. Rev. B 74 (2006) 155201.

[25] D.V. Azamat, A. Dejneka, V.A. Trepakov, L. Jastrabik, M. Fanciulli, V.Y. Ivanov, M. Godlewski, V.I. Sokolov, J. Rosa, A.G. Badalyan, EPR spectroscopy of weak exchange interaction between Co^{2+} ions in ZnO, Phys. Status Solidi 5 (2011) 138–140.

[26] S.K. Misra, S.I. Andronenko, K.M. Reddy, J. Hays, A. Punnoose, Electron paramagnetic resonance of Co^{2+} ions in nanoparticles of SnO_2 processed at different temperatures, J. Appl. Phys. 99 (2006) 08 M106.

[27] T.M. Hammad, J.K. Salem, R.G. Harrison, Structure, optical properties and synthesis of Co-doped ZnO superstructures, Appl. Nanosci. 3 (2013) 133–139.

[28] Y. Hu, H.J. Chen, Preparation and characterization of nanocrystalline ZnO particles from a hydrothermal process, J. Nanopart. Res. 10 (2008) 401–407.

[29] Ch-H. Hsien, Spherical zinc oxide nano particles from zinc acetate in precipitation method, J. Chin. Chem. Soc. 54 (2007) 31–34.

[30] D.A. Azamat, M. Fanciulli, The structure of charge-compensated Fe^{3+} ions in ZnO, Phys. B—Condens. Matter. 401–402 (2007) 382–385.

[31] H. Kaftelen, K. Ocakoglu, S. Tu, R. Thomann, S. Weber, E. Erdem., EPR and photoluminescence spectroscopy studies on the defect structure of ZnO nanocrystals, Phys. Rev. B 86 (2012) 014113.

[32] S.K.S. Parashar, B.S. Murty, S. Repp, S. Weber, E. Erdem, Investigation of intrinsic defects in core-shell structured ZnO nanocrystals, J. Appl. Phys. 111 (2012) 113712.

[33] K. Hoffmann, D. Hahn, Electron-spin resonance of lattice-defects in Zinc oxide, Phys. Status Solidi A—Appl. Res. 24 (1974) 637–648.

[34] T.L. Estle, M. De Wit, Paramagnetic resonance of Co^{2+} and V^{2+} in ZnO, Bull. Am. Phys. Soc. 6 (1961) 445.

[35] P. Koidl, Optical absorption of Co^{2+} in ZnO, Phys. Rev. B 15 (1977) 2493–2499.

[36] A. Abragam, B. Bleaney, Electron Paramagnetic Resonance of Transition Ions, Clarendon Press, Oxford, 1970.

[37] S.K. Misra, in: S.K. Misra (Ed.), Multifrequency Electron Paramagnetic Resonance: Theory and Applications, Wiley-VCH, Weinheim, Germany, 2011.

[38] S.K. Misra, S.I. Andronenko, A. Thurber, A. Punnoose, A. Nalepa, An X-, Q. band, Fe^{3+} EPR study of nanoparticles of magnetic semiconductor $Zn_{1-x}Fe_xO$, J. Magn. Magn. Mater. 363 (2014) 82–87.

[39] T. Dietl, H. Ohono, F. Matsukura, J. Cibert, D. Ferrand, Zener model description of ferromagnetism in zinc-blende magnetic semiconductors, Science 287 (2000) 1019–1022.

[40] X.X. Wei, C. Song, K.W. Geng, F. Zeng, B. He, F. Pan, Local Fe structure and ferromagnetism in Fe-doped ZnO films, J. Phys.: Condens. Matter 18 (2006) 7471–7479.

[41] J.M.D. Coey, A.P. Douvalls, C.B. Fitzgerald, M. Venkatesan, Ferromagnetism in Fe-doped SnO_2 thin films, Appl. Phys. Lett. 84 (2004) 1332–1334.

[42] J.M.D. Coey, P. Stamenov, P.D. Gunning, M. Venkatesan, K. Paul, Ferromagnetism in defect-ridden oxides and related materials, New J. Phys. 12 (2010) 053025.

[43] A. Mauger, No intrinsic ferromagnetism in transition-metal-doped ZnO: an electron paramagnetic resonance analysis received, Appl. Magn. Res. 39 (2010) 3–29.

[44] C. Morhain, C. Deparis, M. Laugt, M. Goiran, Z. Golacki, Magnetic anisotropy of Co^{2+} as signature of intrinsic ferromagnetism in ZnO:Co, Phys. Rev. Lett. 96 (2006) 017203.

[45] S. D'Ambrosio, V. Pashchenko, J.-M. Mignot, O. Ignatchik, R.O. Kuzian, A. Savoyant, Z. Golacki, K. Grasza, A. Stepanov, Competing exchange interaction in Co-doped ZnO: departure from the superexchange picture, Phys. Rev. B 86 (2012) 035202.